Energy 305 (2024) 132327

Contents lists available at ScienceDirect

Energy

journal homepage: www.elsevier.com/locate/energy

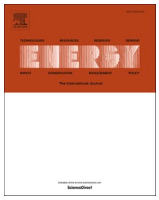

Valorization of cheese-making residues in biorefineries using different combinations of dark fermentation, hydrothermal carbonization and anaerobic digestion

Lidia Lombardi [a], Shivali Sahota [a], Alessandra Polettini [b], Raffaella Pomi [b], Andreina Rossi [b], Tatiana Zonfa [b], Grzegorz Cema [c], Klaudia Czerwińska [d], Aneta Magdziarz [d], Joanna Mikusińska [d], Maciej Śliz [d], Małgorzata Wilk [d,*]

[a] Niccolò Cusano University, Via Don Carlo Gnocchi 3, Rome, 00166, Italy
[b] University of Rome "La Sapienza" (IT), Via Eudossiana 18, Rome, 00184, Italy
[c] Silesian University of Technology, Akademicka 2A, 44-100, Gliwice, Poland
[d] AGH University of Krakow, 30 Mickiewicza Av., 30-059, Kraków, Poland

ARTICLE INFO

Keywords:
Hydrothermal carbonization
Dark fermentation
Cheese whey
Process water
Hydrochar
Biometane potential test

ABSTRACT

Dark fermentation (DF), hydrothermal carbonization (HTC) and anaerobic digestion (AD) are applied, in different combinations, to cheese whey (CW), which is the liquid effluent from the precipitation and removal of milk casein during the cheese-making process. The aim and novelty of this research is to investigate the production of various biofuels (H_2-rich gas, hydrochar and biogas) in cascade, according to the waste biorefinery concept. The simplest case is the direct AD of CW. The second investigated possibility is the preliminary HTC of CW, producing hydrochar, followed by the AD of the process water from which hydrochar is separated by filtration. The third possibility is based on DF of CW, followed by the AD of the fermentate (F) from DF. The final possibility is based on DF of CW, followed by HTC of the F, and then AD of the process water. Accordingly, the physical and chemical properties of CW, F, resulting hydrochar and process water (PW), and biomethane potentials of CW, F, and process waters are studied to determine the energy and carbon balances of all variants. In brief, the first variant, direct AD of CW, is believed to be the most energy efficient method.

1. Introduction

Throughout the last few years, the European Commission (EC) has promoted intense research in the field of bioeconomy, which is founded on the use of renewable biological resources to produce food, materials and energy, and to accelerate progress towards a circular and low-carbon economy [1]. Within this framework, the biorefinery concepts – intended as a chain of processes able to convert biomass into chemicals, materials and fuels [2–5] – and its applications have gained interest and success [6]. Implementing renewable waste streams – or biowaste – where feedstock to biorefinery is generally called the waste biorefinery concept [7], besides any previous advantages, can provide safe and efficient routes for the exploitation of biowaste.

Among the types of biowaste, cheese whey (CW) is an agro-industrial liquid effluent generated by the precipitation and removal of milk casein during the cheese-making process, which is the main by-product of the dairy industry [8], as it plays an important role in the agro-industrial economy of the European Union (EU). Indeed, the EU produced 161.0 million tonnes of raw milk in 2021, of which 71 % of all whole milk available to dairies in the EU is used to make cheese and butter [9]. CW specific production is relatively high and equal to around 9–10 L of CW per kg of produced cheese [10], approximately 57 million (M) tonnes per year in the EU [9]. It is characterized by a rather high organic load of 50–100 g COD/L, which makes it challenging to be processed [11,12] and hazardous to the environment if not properly treated [10].

CW, as other biowastes, can be treated by biological or thermal processes. Among the biological processes, anaerobic digestion (AD) is the most consolidated, with its ability to produce biogas (generally composed of 55–60 % vol. methane and 40−45 % vol. carbon dioxide), which is a renewable fuel. In the case of CW, due to its high organic load

* Corresponding author.
E-mail address: mwilk@agh.edu.pl (M. Wilk).

https://doi.org/10.1016/j.energy.2024.132327
Received 27 January 2024; Received in revised form 5 June 2024; Accepted 4 July 2024
Available online 6 July 2024

Nomenclature

AD	anaerobic digestion	EU	European Union
AMPTS	Automatic Methane Potential Test System	F	fermentate from DF
C	carbon, % wt.	FTIR	Fourier-transform infrared spectroscopy
Ca	calcium, mg/L	HHV	high heating value, MJ/kg
CCE	carbon conversion efficiency, %	HTC	hydrothermal carbonization
COD	chemical oxygen demand, mg/L	H	hydrogen, % wt.
co−HTC	hydrothermal co-carbonization	H_2	hydrogen, % vol.
$C_{in,CW}$	carbon input in 1 kg of dry CW, kg C/kg TS in CW	MECs	microbial electrolysis cells
$C_{in,HTC}$	carbon entering HTC, kg C/kg TS in CW	Mg	magnesium, mg/L
$C_{in,AD}$	carbon entering AD, kg C/kg TS in CW	NH_4–N	ammonium, mg/L
$C_{out,AD}$	carbon exiting from AD, kg C/kg TS in CW	N	nitrogen, % wt. or mg/L
$C_{out,AD,biogas}$	carbon in the biogas from AD, kg C/kg TS in CW	O	oxygen, % wt.
$C_{out,HTC,hydrochar}$	carbon in the hydrochar from HTC, kg C/kg TS in CW	PF	photo fermentation
$C_{out,HTC}$	carbon exiting from HTC, C/kg TS in CW	PO_4–P	phosphate, mg/L
$C_{out,DF}$	carbon exiting from DF, C/kg TS in CW	PW	process water
$C_{out,DF,gas}$	carbon in the DF gas, C/kg TS in CW	TG	thermogravimetric analysis
CSTRs	continuous-flow stirred tank reactors	TGA	thermal analysis
CW	cheese whey, % wt.	TOC	total organic carbon, mg/L
C_6H_5O	phenol, mg/L	TS	total solids
DF	dark fermentation	VFAs	volatile fatty acids,
DSC	differential scanning calorimetry	VS	volatile solids, % wet wt.
DTG	differential thermogravimetric	$VS_{in,CW}$	volatile solids input in 1 kg of dry CW, kg VS/kg TS in CW
ECE	energy conversion efficiency, %	$VS_{in,DF}$	volatile solids entering DF, kg VS/kg TS in CW
EDR	energy density ratio, %	$VS_{out,DF}$	volatile solids exiting from DF, kg VS/kg TS in CW
$E_{in,CW}$	energy input in the form of HHV of dry CW, MJ/kg TS in CW	$VS_{in,HTC}$	volatile solids entering HTC, kg VS/kg TS in CW
$E_{out,AD}$	energy output in the form of methane from AD, MJ/kg TS in CW	$VS_{out,HTC,PW}$	volatile solids exiting from HTC in the PW, kg VS/kg TS in CW
$E_{out,HTC}$	energy output in the form of hydrochar from HTC, MJ/kg TS in CW	$VS_{in,AD}$	volatile solids entering AD, kg VS/kg TS in CW
$E_{out,DF}$	energy output in the form of hydrogen from DF, MJ/kg TS in CW		
E_{out}	$E_{out,DF} + E_{out,AD} + E_{out,HTC,}$ MJ/kg TS in CW		

and low alkalinity, the methane yields might be hindered by volatile fatty acids (VFAs) accumulation and process acidification, resulting in relatively reduced specific methane production in the range 270–600 L/kg VS [10]. In order to manage acidification, the process can be divided into the two-stage type, with the first phase encompassing the hydrolysis-acetogenesis, and the second phase being the methanogenic one, for improving degradation and methane production [10].

Dividing the process into two phases offers the possibility to exploit the first acidogenic one to produce a hydrogen-rich gas (generally composed of 50–55 % vol. hydrogen and 45−50 % vol. carbon dioxide), according to the dark fermentation (DF) process [13]. However, DF cannot stand alone since it has a rather low efficiency [7], producing a liquid effluent – DF fermentate (F) – rich in VFAs, for which a subsequent treatment is required to increase the overall conversion of the organic substance entering the system. Photo fermentation (PF) or microbial electrolysis cells (MECs) or even more complex processes, i.e. biopolymers production, can be applied [13–15]. By simply adding a second AD phase, it allows for the production of conventional biogas, generally with an improved specific biogas production, with respect to the single AD [13].

Among the thermal processes, hydrothermal carbonization (HTC) is suitable for processing organic feedstocks with a high moisture content such as biomass, including sewage sludge [16–19], green waste, lignocellulosic biomass, food and agricultural waste [20,21] and organic fraction from mixed solid waste [22,23]. The application of HTC converts organic feedstock by thermochemical reactions including hydrolysis, decarboxylation, and dehydration into three products: solid, liquid, and gaseous. The solid product is a carbon-like hydrochar with upgraded physical and chemical properties depending on the feedstock origin. The liquid phase, a process water, which is often a major product, may be highly toxic, thus, requires proper management. The gases consist mainly of nitrogen and carbon dioxide, and some combustible gases. The operation of the process is within in the temperature range of 180–350 °C, under autogenous pressure, and above saturation pressure to ensure the liquid state of water. The reaction time takes between one and several hours.

In principle, HTC can be applied to the raw CW or to the F. Hydrothermal co-carbonization (co−HTC) of CW and sewage sludge proved to enhance the fuel properties of hydrochar, with respect to hydrochar obtained from only sewage sludge [24]. CW was processed by HTC, among other substrates, to investigate the extraction by solvent of the secondary char from primary char [25]. Other studies focused on the HTC of wastewater from the dairy industry [26]. Whereas, several works have been published on the possibility of processing different substrates by HTC digestate from AD [27–30], although the application to F is not yet reported in the literature.

In the present work, DF, AD and HTC were applied in various combinations to CW (Fig. 1) with the aim of investigating the production of different biofuels (H_2-rich gas, biogas and hydrochar) in cascade, according to the waste biorefinery concept. The simplest case is the direct AD of CW. The second investigated possibility is the preliminary HTC of CW, producing hydrochar, followed by the AD of the liquid fraction from which hydrochar is separated by filtration (i.e. process water). The third possibility is based on DF of CW, followed by the AD of the F. The final possibility is based on DF of CW, followed by the HTC of the F, and then the AD of the process water. As the chain becomes more complex, different energy outputs are obtained, according to the biorefinery approach: biogas from AD, hydrochar from HTC and H_2-rich gas from DF.

The aims of this work are to:

i) characterize the outputs from each considered process: dark fermentation, anaerobic digestion and hydrothermal carbonization;
ii) compare the chemical and physical properties of dried cheese whey, fermentate and their hydrochars;
iii) compare the anaerobic digestion performance of cheese whey, fermentate and process waters from the hydrothermal carbonization of CW and their main parameters;
iv) compare the different process schemes in terms of energy output.

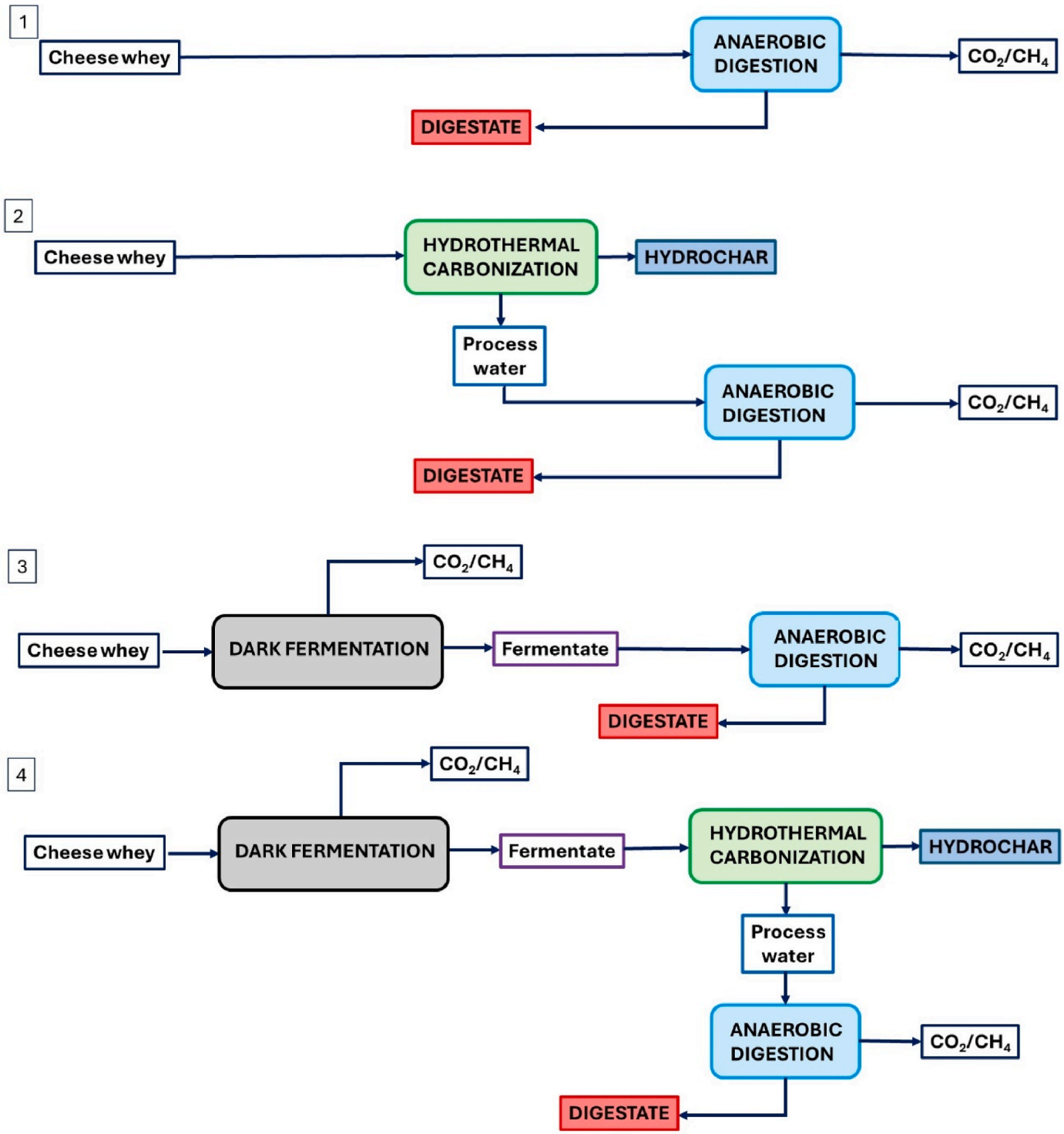

Fig. 1. Schematic concepts of the analyzed processes.

2. Materials and methods

2.1. Materials – cheese whey

CW from the ricotta cheese processing of an Italian dairy industry located in the Lazio Region, was employed as the initial substrate for dark fermentation, hydrothermal carbonization and anaerobic digestion tests. The CW, produced at a temperature of 50 °C, was collected and stored at 18 °C until required. CW characteristics are shown in Table 1. CW samples were shipped to Poland for HTC and AD tests.

Table 1
Characteristics of raw cheese whey.

Parameter	Unit of measurement	Value
Total solids (TS)	% wet wt	10.2 ± 0.1
Volatile solids (TVS)	% wet wt	8.45 ± 0.1
Soluble carbohydrates	g glucose-C/L	82.0 ± 1.0
Total organic carbon	g C/L	49.6 ± 1.6
pH	–	3.4 ± 1.0

2.2. Methods

2.2.1. Dark fermentation

2.2.1.1. Experimental tests. Frozen CW samples were thawed at 4 °C when required for use at the experimental stage.

The fermentative H_2 production tests were performed in continuous-flow stirred tank reactors (CSTRs) with a working volume of 0.5 L (50 % of the reactor volume). A total of eight replicates were performed in batch mode to guarantee accuracy and preciseness of the experimental results and to collect adequate amounts of fermented material for use in the subsequent treatment stages. The obtained F samples, still rich in organics, were shipped to Poland for HTC and AD tests.

During the startup phase, the reactors were flushed with N_2 (with a volume of ~1 L) to ensure anaerobic conditions.

The stirring was retained at 500 rpm and the temperature was maintained under mesophilic conditions (38 ± 1 °C) using a heating plate combined with a magnetic stirrer.

No inoculum was added during the process, as the indigenous microorganisms in CW were able to produce H_2 through dark fermentation, as shown in previous studies [11,13].

In order to avoid acidification, NaOH was added at a concentration of 2 M by means of an automated system that was preset to maintain the pH value of 6 throughout the process. There was no acid addition when the pH value increased to above 6 since the shift, which reached a pH value of 6.9, did not cause noticeable alterations to the H_2 production process.

2.2.1.2. Analytical methods. The gas production was measured through a volumetric gas counter with a capacity of 2 mL (Gas Endeavour® from Bioprocess Control), which was, in turn, connected to gasbags for gas storage. The gas was periodically sampled from the gasbags with a gastight syringe (25 mL) and analyzed using a gas chromatograph (Model 3600 CX, VARIAN) equipped with a thermal conductivity detector and 2−m stainless−steel packed column (ShinCarbon ST) with an inner diameter of 1 mm. The injector and detector operate, respectively, at a temperature of 100 °C and 130 °C. Helium gas was employed as the carrier. The oven temperature was increased from 80 °C to 100 °C at 2 °C/min.

The measured volume was converted under standard pressure and temperature conditions (T = 273.15 K, P = 100000 Pa); thus, all the gas properties are referred to as standard conditions.

Total solids (TS) and volatile solids (VS) were measured according to the Standard Methods for the Examination of Water and Wastewater [31]. Total organic carbon (TOC) was measured through the Shimadzu TOC analyzer (TOC−VCHS and SSM−5000 module, Shimadzu, Japan). Soluble carbohydrates were analyzed with a spectrophotometer through the colorimetric phenol–sulphuric acid method, using glucose as the standard [32].

2.2.2. Hydrothermal carbonization

2.2.2.1. Experimental tests. Hydrothermal carbonization experiments were conducted, using CW and F samples in a Zipperclave Stirred Reactor (Parker Autoclave Engineers, USA) equipped with a Magne-Drive stirrer. The reactor has a volume of 1000 cm^3 and operates with temperatures under 232 °C and pressure below 15.1 MPa. It has a removeable electric heating mantle, and a built-in cooling coil which allows for immediate cooling down of the reactor after the process. The control panel provides for and monitors online heat and process temperatures, pressures and rotations per minute for the stirrer speed. The experimental procedure was as follows: firstly, 250 g of the sample was inserted into the vessel then the reactor was closed. To ensure high pressure during the process, the reactor was flushed with argon gas to remove air at a flow rate of 5 L/min. Then the outlet was closed to increase pressure in the reactor up to 4 bar. Next, the reactor was sealed and the argon flow was discontinued. Then the heating mantle was clipped to the reactor and activated. The desired temperatures of 200 and 220 °C, and 180 °C performed only for F, was reached after c.a. 1 h and maintained for 2 h of reaction time. When the reaction time finished, the heating mantle was removed, and cooling of the reactor was conducted through a built-in coil. When room temperature was reached, the HTC gaseous sample was collected and placed in a Tedlar bag for further chemical analysis. Then, the reactor was opened and the post-processing mixture was evacuated and separated via a filtration process through a vacuum filtration apparatus consisting of filtration paper, a Buchner's funnel and flask. The solid fraction, hydrochar, was dried in the dryer at 105 °C for 24 h and the filtrated liquid fraction, process water (PW), was stored at 4 °C in the refrigerator. The HTC tests were triplicated for every condition of the process. In order to estimate the HTC product distribution, the feedstock and hydrothermally treated material were weighed at every stage of the experiments. Firstly, prior to and after the HTC process, the feedstock and resulting slurry were measured to estimate the amount of produced gas. The complete evacuation of slurry from the reactor is very difficult to achieve because some liquid and solid particles remain on the reactor wall hence the gas fraction is reported together with losses. Then the solid and liquid fractions are separated by the filtration process and both weighed. By using this method a distribution of the HTC product is assessed. In addition, the mass yield of hydrochar is calculated as the ratio of dry mass of hydrochar compared to the dry mass content of the feedstock before the experiment. The energy yield is the mass yield multiplied by the energy densification ratio, which is the ratio between the higher heating value (HHV) of hydrochar and the untreated solid fraction.

HTC tests were labelled according to the used substrate, CW or F, the process temperature (180, 200 or 220 °C), the reaction time (2 h) and the number of replications (1, 2 or 3), for instance: CW_220_2 h_1. Overall, 15 tests were performed (3 replications of 5 conditions).

2.2.2.2. Analytical methods for solid samples

2.2.2.2.1. Ultimate analysis. The ultimate analysis (hydrogen, carbon, nitrogen and sulphur content) was performed on a Leco Elemental Analyzer (CHNS628) according to the PKN–ISO/TS 12902:2007 standard. For the determination of carbon, hydrogen, and nitrogen, the combustion process was conducted at 950 °C, whereas for sulphur, it was 1350 °C, in an oxygen atmosphere. The presence of CO_2, H_2O and SO_2 was detected with infrared light. For nitrogen content analysis, a thermal conductivity detector was used. The oxygen content was determined, by difference, taking into account CHNS, moisture and ash content.

2.2.2.2.2. Proximate analysis. The 5 E-MAC6710 Proximate Analyzer (Thermogravimetric Analyzer, TGA) was operated according to ASTM D7582 (Standard Test Methods for Proximate Analysis of Coal and Coke by Macro Thermogravimetric Analysis) and ISO 17246:2010 (Coal – Proximate analysis) for feedstocks, hydrochar derived from CW at 200 and 220 °C and F at 180 °C to determine moisture, ash and volatile contents. In the case of hydrochar derived from F at 200 and 220 °C, ash contents were determined as a residue from TGA due to the small amount of samples.

2.2.2.2.3. Thermal analysis. Thermogravimetric analysis of the hydrochar was performed using the TGA/DSC analyzer at 10 K/min of heating rate, up to 800 °C, under atmospheric air. During the linear increase in temperature, the mass change was recorded continuously in the form of TG curves (thermogravimetry), and the heat effects in the form of the DSC curve. The TG curve describes the change in mass of the tested material depending on the temperature m = f(T) for the given measurement conditions (heating rate, atmosphere). DTG curves were obtained as a result of mathematical transformations (differentiation of the TG curve as a function of temperature): dm/dT = f(T). The DTG curve ensures that it is easier to distinguish and separate weight loss under similar conditions, which on the TG curve may be unnoticed. The

maximum rate of mass change corresponds to the tip of the peak. Additionally, the moisture and solid residue from TGA were determined for CW, F, and their hydrochar performed at 200 and 220 °C to calculate oxygen content and HHV and to assess the convergence between the methods.

2.2.2.2.4. Higher heating value. HHVs of the samples (CW and F) were calculated by using Parikh and Channiwala [33] based on the elemental composition and ash content:

$$HHV = 0.3491 \cdot C + 1.1783 \cdot H + 0.1005 \cdot S - 0.1034 \cdot O - 0.015 \cdot N - 0.0211 \cdot Ash \quad (1)$$

This equation was used due to the low mass of the sample as other analytical methods require greater amounts. However, HHV was experimentally determined for two samples which were in higher quantity (CW_HTC_220_2 h and CW_HTC_2200_2 h) using the Leco AC500 isoperibolic calorimeter according to DIN 51900 and ISO 1928 standards, to assess the convergence between the methods.

2.2.2.2.5. FTIR. The functional groups in the studied samples were identified by FTIR spectroscopy by means of a Bruker Alpha II system (Bruker Optics Inc., USA) within the infrared absorption frequency range: 400–4000 cm^{-1}.

2.2.3. Analytical procedures for liquid fraction

2.2.2.3.1. Physical and chemical analyses. PW derived from the HTC process, were analyzed in order to evaluate the treatment effect on the pH value and conductivity, which were monitored by the multifunctional analyzer CX–461 (Elmetron, Zabrze, Poland). Additionally, the chemical oxygen demand (COD), total organic carbon (TOC), concentration of Phenol (C_6H_5O), Phosphate (PO_4–P), Amonium (NH_4–N), Calcium (Ca), Magnesium (Mg), and Nitrogen (N) were determined using a Spectrophotometer Merck Spectroquant Prove 100 and Thermoreactor Merck Spectroquant® Series TR 420, according to the manufacturer's instructions. Ultimate analysis was conducted by the Elemental Analyzer Leco CHN 628.

2.2.3. Anaerobic digestion

2.2.3.1. Bomethane potential tests. The AMPTS II (Automatic Methane Potential Test System) from Bioprocess Control was utilized to assess the biomethane potential of selected samples: CW, F, PW obtained from filtration of the slurry left by HTC at 200 °C of CW (CW_PW_200), PW obtained from filtration of the slurry left by HTC at 200 °C of F (F_PW_200). The AMPTS system comprises three units [34]. Biogas production was directly measured online using the liquid displacement and buoyancy method. Prior the test, the VS, COD, and pH of the total inoculum and the tested samples were measured, and the inoculum was mixed with the test samples based on this measurement. In order to ensure proper BMP testing, an inoculum−to−substrate (I/S) ratio of 3 was assumed (based on VS), since a ratio of 2 − 4 is required [35]. The tests were performed in 500 mL reactors with a useable volume of 400 mL and 150 mL of gas space (including the reactor, tubing, and NaOH bottles). Additionally, a blank test was conducted to assess the inoculum's methane production productivity. The reactors were purged with nitrogen gas for 1 min and then incubated at 37 °C under mesophilic conditions until daily gas production dropped below 5 NmL/d, following the procedure established by Lehtomäki et al. [36].

2.2.4. Energy yields and carbon balance

Applying the results obtained from the experimental tests (average values of the tests at different conditions which concerns HTC), the energy outputs (i.e. DF H_2-rich gas, AD biogas and hydrochar from HTC) were calculated for the four chains as depicted in Fig. 1. The calculation was made in reference to 1 unit of mass (i.e. 1 kg) of TS entering with the CW, while also considering the amount of TS/VS transformed by each process of the chain, thus assuming that the amount of TS/VS exiting from one of the process units is the input to the following one. Energy output was calculated based on the HHV of produced fuels, on a dry basis.

The energy conversion efficiency (ECE) was calculated according to the following:

$$ECE\ [\%] = (E_{out,H2} + E_{out,CH4} + E_{out,HC}) / E_{in,CW} \cdot 100 \quad (2)$$

where:

$E_{out,H2}$ is the energy output in the form of hydrogen from DF, expressed in [MJ/kg TS in CW].

$E_{out,CH4}$ is the energy output in the form of methane from AD, expressed in [MJ/kg TS in CW].

$E_{out,HC}$ is the energy output in the form of hydrochar from HTC, expressed in [MJ/kg TS in CW].

$E_{in,CW}$ is the energy input in the form of HHV of dry CW, expressed in [MJ/kg TS in CW].

Similarly, based on the available characterization, in terms of C content, and the entering and exiting streams from each process unit, a carbon balance was drafted, to gain a better understanding of how C is used/converted by the different processes.

The carbon conversion efficiency (CCE) was calculated according to the following:

$$CCE\ [\%] = (C_{out,H2} + C_{out,CH4} + C_{out,HC}) / C_{in,CW} \cdot 100 \quad (3)$$

where:

$C_{out,H2}$ is the carbon in the DF gas, expressed in [kgC/kg TS in CW]; even if this C is all in the form of CO_2 (thus, not a useful product), it was included as useful conversion of C (i.e. numerator of the defined efficiency), and as being an unavoidable co-product of H_2;

$C_{out,CH4}$ is the carbon in the biogas from AD, expressed in [kg C/kg TS in CW]; similarly including C in the form of both CH_4 and CO_2 in the biogas;

$C_{out,HC}$ is the carbon in the hydrochar from HTC, expressed in [kg C/kg TS in CW].

$C_{in,CW}$ is the carbon input in 1 kg of dry CW, expressed in [kg C/kg TS in CW].

Details on TS, VS, C and energy calculations are reported in Supplementary Material.

3. Results

3.1. Dark fermentation process

Table 2 depicts the results in terms of average values obtained from the eight batch tests expressed as H_2 yield and H_2-rich gas yield with respect to TOC or TS content in the raw CW. The H_2-rich gas is a mixture of H_2 and CO_2 and its composition is reported. The volume of NaOH added during the tests, and the TS content in the F are also shown. It can

Table 2
NaOH dosages, H_2 and biogas yields and F properties from the CW dark fermentation tests (average values of 8 replicates).

Parameter	Unit of measure	Value
H_2-rich gas yield	L/kg TOC	312.1 ± 69.3
	L/kg TS	151.6 ± 33.6
H_2-rich gas composition	% vol. H_2	43 ± 3
	% vol. CO_2	57 ± 3
H_2 yield	L H_2/kg TOC	135.5 ± 34.2
	L H_2/kg TS	65.80 ± 16.63
Amount of NaOH added throughout the fermentation process	L NaOH/kg CW	0.355 ± 0.033

be noted that, at the end of the test, the F includes both the fermented CW and the added NaOH.

3.2. Hydrothermal carbonization process

During the HTC process, the reactor temperature and pressure were continuously controlled in order to monitor the process evolution and maintain stable conditions. The samples of CW had a very specific odour, which became less intensive after the treatment. The bright yellow colour of the CW changed to a warm brown colour as a result of the carbonization process. One of the most significant effects of the HTC process, which should be highlighted, was the increased settleability of the solids that were easily separated from the liquid phase. Prior to the HTC process the solid fraction proved to have poor settling properties and the filtration process was hindered by the clogging of filters critical clogging. Conversely, after HTC, the solid and liquid fractions were easily separated, as confirmed by preliminary studies [37].

3.2.1. Solid and liquid material characteristics

The initial TS for feedstock samples for CW and F was 10.2 % and 7.7 %, respectively. Therefore, in all the studied cases and due to a high dilution of feedstocks the major product of the HTC process was liquid at over 86.05 – 96.25 %, then gas and losses c.a. 3.7 – 9.93 %, and the lowest quantity, ca. 0.05 – 4.18 %, presented as hydrochar (Table 3). The very low mass efficiency of hydrochar is also confirmed by Pecchi et al. [25], who found that the hydrochar yield for CW was the lowest among the tested materials, i.e. a mixture of food waste, dairy cheese whey and brewer's grain.

The results of the elemental analysis of dry feedstocks and hydrochar are summarized in Table 4. In general, HTC caused an increase in carbon, nitrogen and sulphur contents in hydrochar from CW confirming that the carbonization process occurred. Carbon contents increased approximately 45 % for hydrochar which corresponded with an increase of HHVs around 45 %. Overall, the change of temperature had only a slight effect on the carbon contents and HHVs. Conversely, hydrochar from F behaved differently. Hydrogen increased and nitrogen decreased besides the carbon which slightly increased. Sulphur content was measured only for F and F_220_2 h_3 hydrochar indicating that its amount was at a very low level, far beyond 0.1 % and could be neglected.

HHVs were determined using ash content either by a proximate analyzer or by TGA as a residue for CW, F and hydrochar. Both methods confirmed a significant convergence for all samples (c.a. 0.03 %). In the case of hydrochar derived from F at 200 and 220 °C, and due to the small sample size, only the TGA method was applied, during which both samples exhibited sticking properties to the walls of the crucible and sensor. For hydrochar derived at 180 °C, only the proximate analyzer was used. In addition, the HHV was determined by a calorific bomb for two samples, CW_220_1 and CW_200_2, which provided quite similar results (up to c.a. 3.5 %) proving that the determination of HHV by Eq. (1) was reliable. In connection with CW, the calorific value of 19.76 MJ/kg is similar to the values obtained by Petrovi et al. [24] (18.37 MJ/kg) and Pecchi et al. [25] (18.5 MG/kg). Finally, the HHV using ash content and determined by TGA was used for energy balance.

Table 3
HTC product distribution.

HTC Sample	Solid fraction, %	Liquid fraction, %	Gas and losses, %
CW_220_2 h_1	3.95	87.54	8.51
CW_220_2 h_2	4.02	86.05	9.93
CW_220_2 h_3	4.18	87.25	8.57
CW_200_2 h_1	3.96	91.45	4.58
CW_200_2 h_2	4.02	91.20	4.78
CW_200_2 h_3	4.06	87.64	8.30
F_220_2 h_1	0.05	96.25	3.70
F_220_2 h_2	0.14	95.68	4.18
F_220_2 h_3	0.58	93.42	6.00
F_200_2 h_1	0.44	92.38	7.18
F_200_2 h_2	0.41	93.91	5.67
F_200_2 h_3	0.20	93.11	6.68
F_180_2 h_1	0.45	92.70	6.84
F_180_2 h_2	0.88	94.05	5.06
F_180_2 h_3	0.83	93.12	6.05

Mass and energy yields of hydrochar derived from CW resulted in around 37 – 39 % and 54 – 57 %, whereas in the case of hydrochar derived from F the results were very poor for mass yield, up to 10 %, and for energy yields, up to 11 %. Additionally, due to high dilution, repeatability of the mass collection was rather poor. Slightly higher energy yields after the HTC process were found by Petrovič et al. [24], who provided a mixture of CW with sewage sludge to the HTC process and recorded a significant increase in energy yields, up to over 75 %. Furthermore, the hydrochar yield improved from 57.10 % for HTC of sewage sludge when compared to 64.14 wt% determined for hydrochar derived from a mixture of sewage sludge with CW.

It was also noticed that the average ash content increases with an increase in the temperature of the HTC process regarding CW and F. The increased ash content with temperature is probably mainly due to mineral retention and loss of volatiles because of decomposition and transformation of organic matter through hydrolysis, dehydration, decarboxylation and deamination [24,38].

Table 5 summarizes the main parameters of liquid samples (CW and F, and PWs after HTC): pH, conductivity, TOC and COD. Initial TOC of CW decreased approximately 2.5 times in PWs of hydrothermally carbonized CW at 200 and 220 °C. However, in the case of F and its PWs the TOC was not affected, but COD was higher at about 25 %. The condition of the HTC process slightly increased the conductivity of PWs for both feedstocks. Moreover, pH values were not affected by HTC in connection with CW, but regarding F it was slightly increased.

In addition, other trends affected by the HTC process were observed in the chemical composition of the liquid phase (Table 6). For instance, the phenol content increased ca. 37 times and 30 times in process waters derived from hydrothermally treated CW at 200 °C and 220 °C versus CW. In the case of PW derived from F it increased about 2 times. For phosphate, it slightly increased for both cases. Calcium decreased significantly about 2 times, but this value was very low for F and its hydrochar. For magnesium, adverse trends were observed, it increased c.a. 2 times. For all hydrochar samples calcium decreased 5 to 7 times when compared to feedstocks. In connection with ammonium, hydrothermal treatment generated an increase of 38–58 % for hydrochar derived from CW, whereas for hydrochar from F the value increased up to 60 %. Nitrogen also increased slightly in both cases. In almost all CW_PWs, the concentration of nitrate was higher than that of ammonium, which is consistent with the results of previous studies [39]. The increase in temperature raised the N content in the CW_PWs, reaching a maximum concentration of 1075 mg/L. The increase in the content of inorganic N with a gentle increase in temperature can be attributed to two main pathways, the first of which is the breakdown of solid nitrogen structures under the influence of an increase in temperature and the second one is suggested by the hydrolysis of Protein N to inorganic N under the influence of a slight increase in temperature HTC [40].

3.2.2. Thermal analysis

The combustion process of the CW and F and their hydrochar derived from the same conditions, 200 °C and 220 °C and 2 h, was conducted by thermal analysis and depicted in the form of TG and DTG curves (Figs. 2 and 3). The combustion process of all the samples were divided into three stages, moisture release, main combustion process, and char combustion. The hydrothermal effect is seen in the thermal behaviour of studied samples. CW started to convert at lower temperatures (DTG peaks – 198 °C, 313 °C) and finished at 550 °C with 8.6 % solid residue. Regarding the thermal behaviour of CW hydrochar (based on TG curves) it can be noticed that there are no significant differences between the stages. Their final residue was the same around 2.5 %.

Table 4
Physical and chemical properties of feedstocks and hydrochar.

Sample	C, %	H, %	N, %	S,%	Ash, %	HHV, MJ/kg	EDR	mass yield, %	energy yield, %
CW	45.80	6.15	2.73	0.14	9.93	19.76	–	–	–
CW_220_1	66.50	6.25	3.68	0.24	3.30	28.62	1.46	36.81	53.31
CW_220_2	66.60	6.23	3.77	0.24	3.30	28.65	1.46	37.46	54.30
CW_220_3	66.50	6.21	3.71	0.24	3.30	28.57	1.46	39.00	56.38
CW_200_1	66.50	6.55	3.90	0.27	2.27	28.88	1.47	36.95	54.00
CW_200_2	66.30	6.36	3.80	0.27	3.79	28.65	1.46	37.46	54.31
CW_200_3	63.16	6.03	3.85	0.28	3.13	27.00	1.38	37.85	51.71
F	34.30	6.20	1.44	0.03	26.08	16.65	–	–	–
F_220_1	60.46	9.31	0.77	–	–	–	–	0.59	–
F_220_2	55.02	8.84	0.93	–	23.46	28.13	1.67	1.53	2.56
F_220_3	55.64	9.04	1.00	0.05	23.46	28.68	1.70	6.60	11.24
F_200_1	52.65	8.07	0.76	–	23.58	24.87	1.56	4.94	7.69
F_200_2	53.95	8.54	0.65	–	23.58	26.05	1.63	4.69	7.64
F_200_3	56.40	8.76	0.75	–	–	–	–	2.30	–
F_180_1	50.96	8.09	1.02	–	25.56	26.81	1.55	5.14	8.28
F_180_2	47.18	7.36	0.98	–	24.35	22.97	1.38	9.99	13.79
F_180_3	44.19	6.36	0.74	–	32.26	20.80	1.25	9.35	11.68

Table 5
Liquid phase analytical results.

Liquid sample	pH	Conductivity, mS/cm	TOC, mg/L	COD, mg/L
CW	3.32	11.9	45800	127300
CW_PW_220_1	3.49	14.7	17525	49870
CW_PW_220_2	3.52	14.9	17925	48935
CW_PW_220_3	3.59	15.1	17800	51000
CW_PW_200_1	3.26	14.2	18725	54040
CW_PW_200_2	3.23	13.8	16950	51600
CW_PW_200_3	3.31	14.5	18000	51625
F	7.77	32.7	12720	86210
F_PW_220_1	8.21	33.0	27875	85325
F_PW_220_2	8.60	33.7	26850	94625
F_PW_220_3	8.21	34.1	26025	92750
F_PW_200_1	8.43	33.8	28900	102025
F_PW_200_2	8.36	33.4	28125	96400
F_PW_200_3	8.27	33.7	28600	107600
F_PW_180_1	8.37	33.9	27975	104700
F_PW_180_2	8.43	34.1	29325	101250
F_PW_220_1	8.41	33.8	28650	103500

Table 6
Phenol, phosphate, ammonium, calcium, magnesium and nitrogen contents.

Liquid sample	C_6H_5OH, mg/L	PO_4–P, mg/L	NH_4–N, mg/L	Ca, mg/L	Mg, mg/L	N, mg/L
CW	3.25	632.5	108	10.3	47.0	863
CW_PW_220_1	118.75	775.0	163	4.8	99.0	975
CW_PW_220_2	120.25	765.0	170	6.0	97.3	1000
CW_PW_220_3	117.38	915.0	168	8.1	153.8	1075
CW_PW_200_1	100.13	767.5	150	6.2	93.8	938
CW_PW_200_2	105.88	723.8	148	5.8	81.5	813
CW_PW_200_3	111.00	837.5	148	5.8	100.8	1050
F	26.00	287.5	388	<1	26.0	1100
F_PW_220_1	46.50	296.3	155	<1	42.8	1525
F_PW_220_2	46.50	255.0	465	<1	38.0	1550
F_PW_220_3	46.25	248.8	488	<1	32.5	1663
F_PW_200_1	53.38	447.5	638	1.8	60.0	1850
F_PW_200_2	51.88	476.3	538	<1	59.8	1650
F_PW_200_3	52.25	478.8	558	<1	64.8	1700
F_PW_180_1	41.63	373.8	620	<1	46.8	1688
F_PW_180_2	44.50	305.0	575	<1	44.3	1775
F_PW_180_3	40.13	286.3	595	<1	43.5	1763

In the case of F, the final residue was much higher c.a. 45 %, hydrothermal treatment caused a decrease ca. 50 % indicating that the higher temperature (220 °C) of the process caused lower solid residue. The character and shape of the combustion profiles of F and its hydrochar differed, up to 350 °C. The maximum heating rate of all F and its hydrochar was maintained within the same range of temperature approximately 490 °C. However, after 500 °C there is no observed mass loss for any of them.

3.2.3. FTIR

FTIR analysis depicted in Figs. 4 and 5 presents a comparative analysis of numerous peaks corresponding to the individual chemical bonds detected in CW, F and their hydrochar. There are two regions with the most significant peaks namely, 3000 − 2800 cm^{-1} and 1800 − 600 cm^{-1}. The first one is assigned as fats and oils region, whereas the second is associated with polysaccharides and carbohydrates. Firstly, in CW and F, there are bonds in the range of 3400 − 3200 cm^{-1} representing O–H as water, which are degraded in hydrochar proving that hydrolysis took place. Then, in the range 3200–2900 cm^{-1} in hydrochar, there occurs higher and more intensive peaks of C–H stretching vibrations of carbonyl groups of triglycerides and stretching vibrations of –C–H(CH_2) and –C–H(CH_3) groups of fatty acids in comparison to CW and F. In the second region, between 2800 and 1800 cm^{-1} there were no particular differences recorded. The C═O stretch of ester or carboxylic acid group assigned as fatty acids at 1740 cm^{-1} is present in CW, but appears weakened in hydrochar and was not observed either in F or its hydrochar. In the range 1700 − 1200 cm^{-1}, there were vibrational bands of fatty acids, proteins and polyssacharides in the dairy products. Concerning the F sample, the highest peak of peptide bonds (CO–NH) is found at 1554 cm^{-1} and of amide C–N at 1406 cm^{-1} [41]. However, they were less intense for F hydrochar. For CW, the highest peak was detected at 1038 cm^{-1}, which was probably assigned for the O–H stretch of carbohydrates such as lactose. This bond was significantly degraded in hydrochar derived from CW at 220 °C as well as all peaks in the region of 1450 − 600 cm^{-1}.

3.3. Biomethane potential test

Table 7 depicts the results of VS, for the tested substrates before the test and the VS, COD and pH for the used inoculum.

CW and its HTC PWs had a very low pH equal to 3.32 and 3.26, respectively. In the case of CW, such a low pH signifies that it can be treated as an acid CW. Compared to sweet CW (pH between 6 and 7), it contains less protein and also has a high salt content [42].

Fig. 6 shows specific methane production per g VS, while Fig. 7 indicates daily methane production as a % of total (cumulative) production.

The F sample exhibited the highest measured methane potential of 724.8 NmL/g VS, while the F_PW_200 sample had a methane potential of 649.5 NmL/g VS. The CW_PW_200 and CW samples had lower methane potential values, with 484.4 and 492.1 NmL/g VS, respectively,

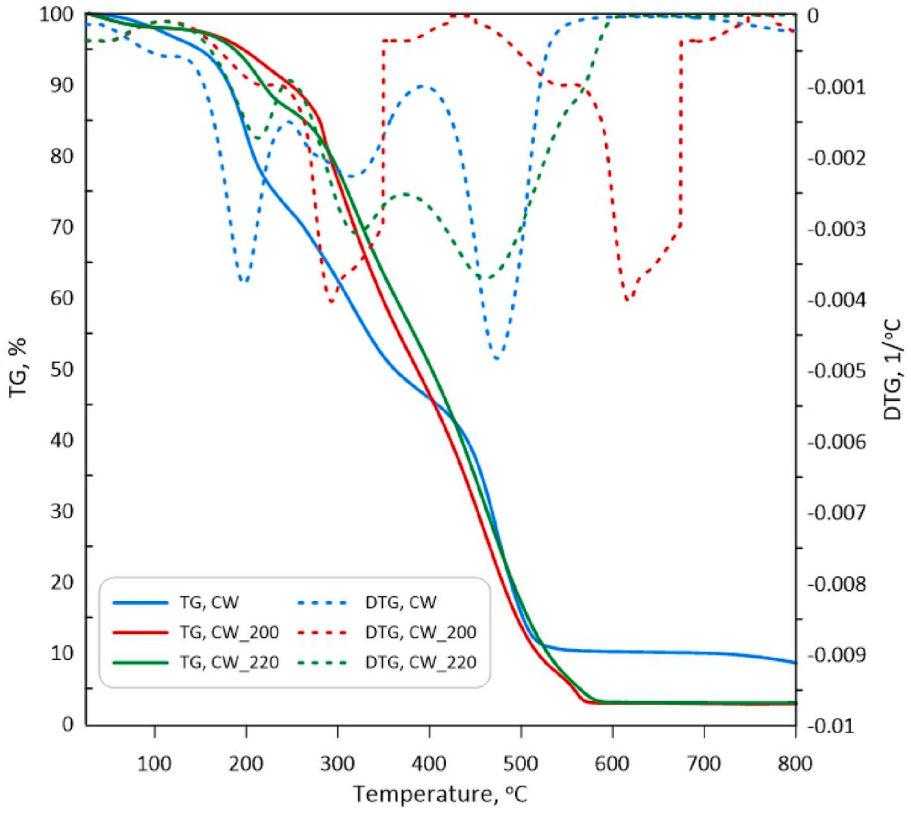

Fig. 2. TG/DTG for CW, CW_200 and CW_220.

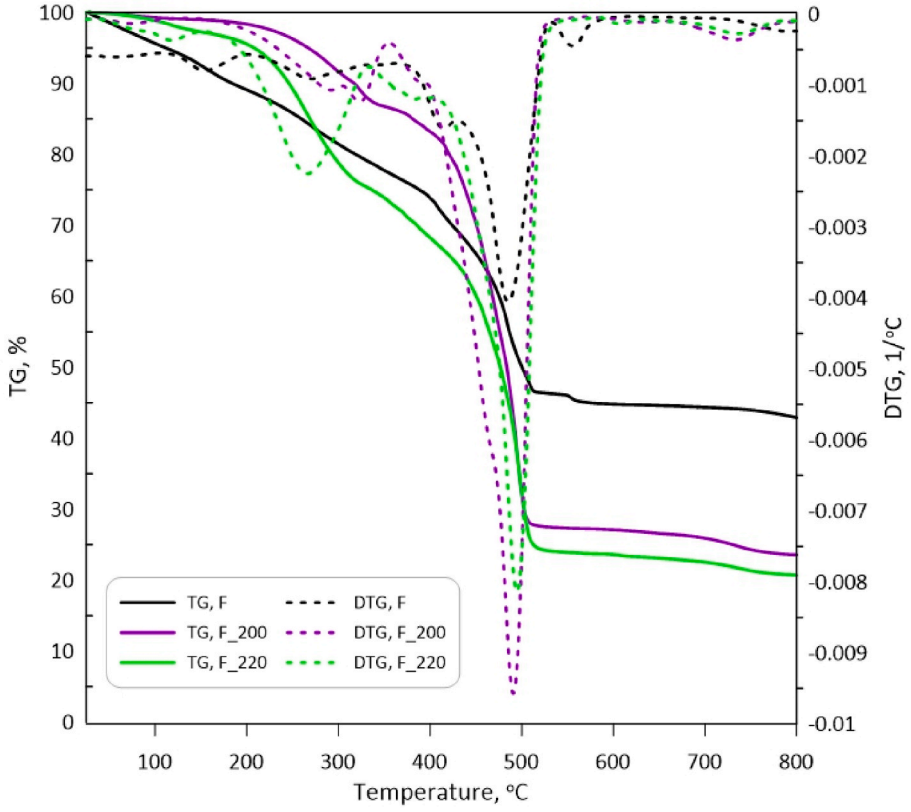

Fig. 3. TG/DTG for F, F_200 and F_220.

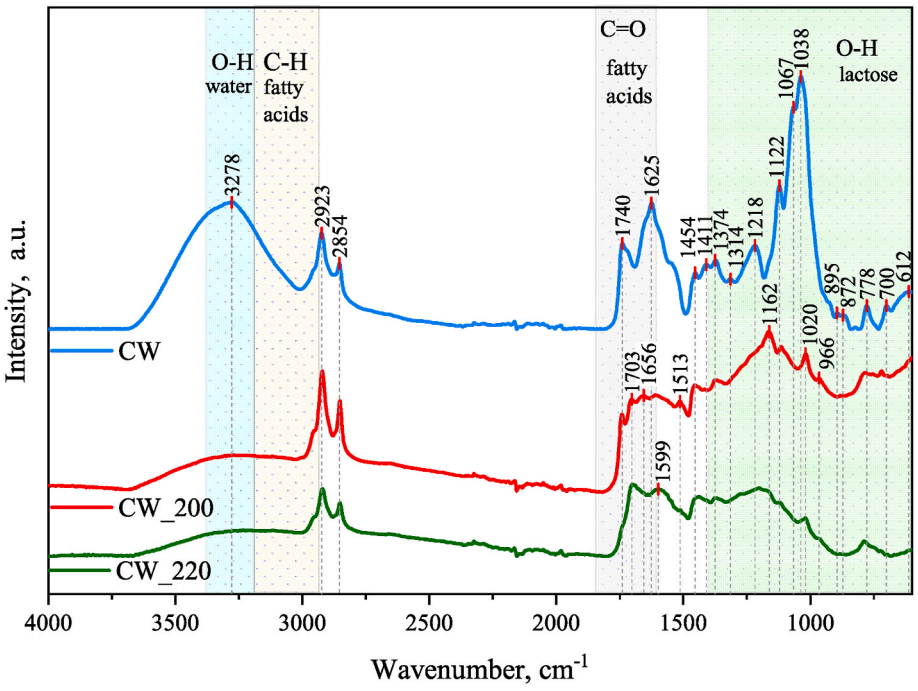

Fig. 4. FTIR results for CW and its hydrochar.

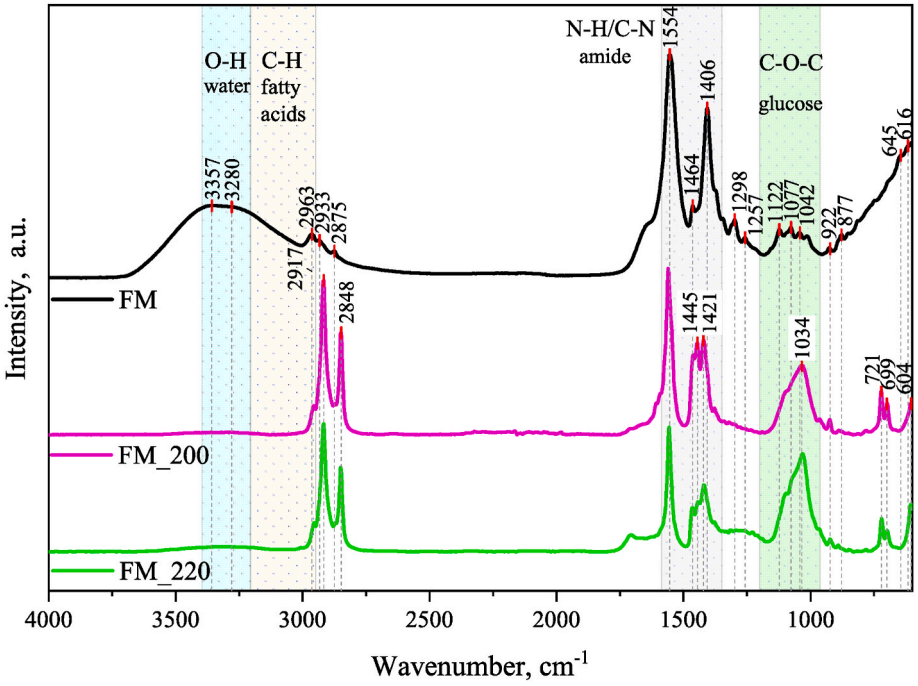

Fig. 5. FTIR results for F and its hydrochar.

Table 7
Results of VS measurements before the test. Inoculum characterization.

	Inocolum	F	F_PW_200	CW	CW_PW_200
VS, %	1.80	4.06	4.05	9.10	2.35
pH	7.04	7.77	8.35	3.32	3.26

although these values were still relatively high (Fig. 6A).

Fig. 7 shows the percentage of biomethane produced per day out of the total amount produced during the test. For the F, F_PW_200, and CW samples, more than 90 % of the methane was produced in the first 10 days of the test. However, the CW_PW_200 sample was an exception, with only 53.3 % of methane produced in the first 10 days. This was due to the low pH of the sample, which caused acidification of the test sample to a level of 5.82 ± 0.04. In order to address this issue, the pH was corrected to 6.84 ± 0.03 with 10 % NaOH. Despite this correction, a lag-phase was observed at the beginning of the test for this sample (Fig. 7A). Nevertheless, the methane potential of the CW_PW_200 sample was comparable to that of the CW sample in the end.

Overall, the CW samples exhibited the fastest methane growth, with

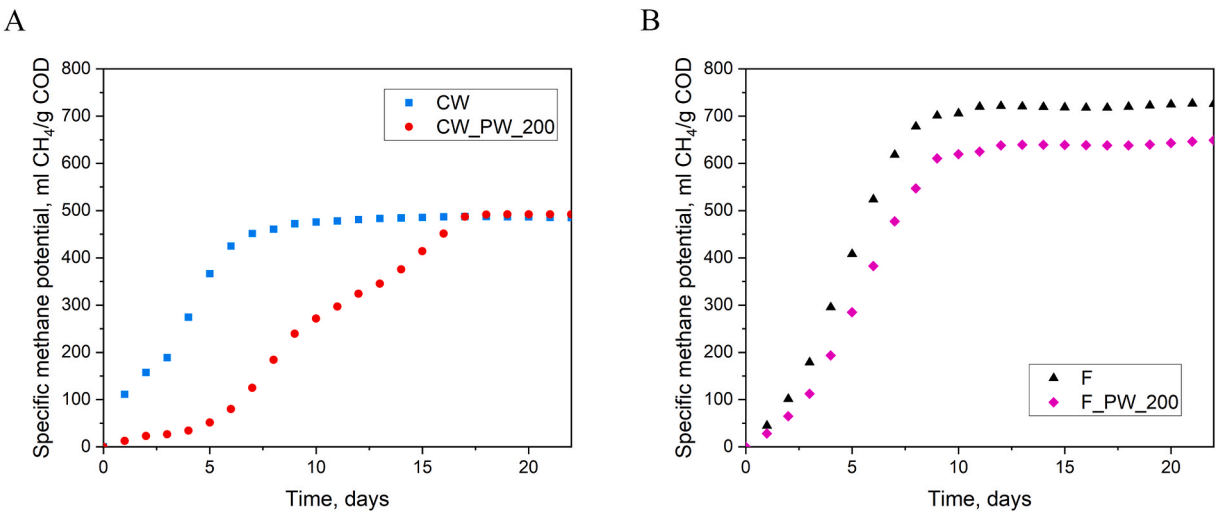

Fig. 6. Specific methane potential A) CW and its HTC process water at 200 °C (CW_PW_200) and B) F and its HTC process water at 200 °C (F_PW_200) A.

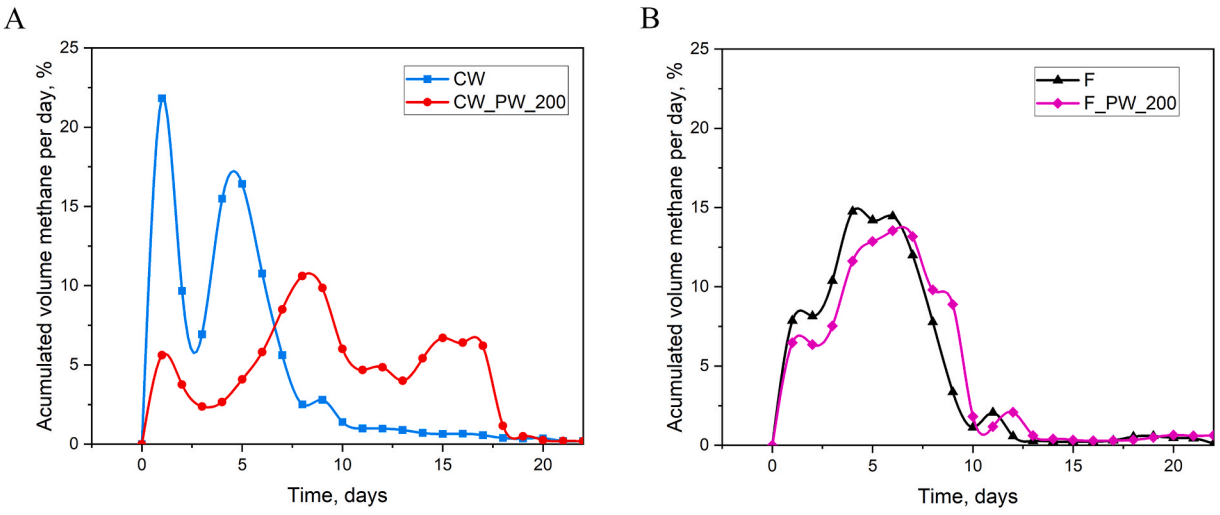

Fig. 7. Daily methane production in relation to total production A) CW and its HTC process water at 200 °C (CW_PW_200) and B) F and its HTC process water at 200 °C (F_PW_200).

the initial peak observed on the first day of the test (21.8 %), followed by a second peak between days 4 and 5. Moreover, the maximum methane potential for CW was achieved within 15 days (Fig. 6A), which is consistent with the findings of Labatut et al. [43]. This is likely due to the fact that CW is primarily composed of easily degradable sugars. Comparable outcomes were observed for the F and F_PW_200 samples, with the highest production also recorded between days 4 and 8 of the test (Fig. 6 B). The measured methane potential of CW falls within the range reported in literature (270 – 600 L/kgVS) [10], and specifically by other researchers: 510 – 600 mLCH_4/g Vs added [44], 423.6 mLCH_4/g VS added [43], and 350 mLCH_4/g VS added [45]. A very similar potential was observed for CW after the HTC process. However, a significantly higher potential was achieved for F and F_PW_200 samples, with the former confirming literature findings [10]. This could be due to the potential production of a large amount of VFAs, which can cause a decrease in pH. This may be the reason why two methane production peaks were observed for the CW sample. In general despite having a high organic matter content, CW's methane yield is restricted due to the production of volatile fatty acids (VFAs) during lactose fermentation [44]. One possible solution to these problems may be, for example, separating acidogenesis from methanogenesis in a two-stage process or simply using CW for hydrogen production [46]. Such a process will greatly limit the issue of acidification during methane fermentation while the effluent from hydrogen fermentation will still contain significant amounts of organic matter. In the present work, the highest methane potential was obtained precisely for the effluent from CW dark fermentation.

3.4. Energy yields and carbon balance

Table 8 depicts the energy outputs per unit of mass of entering TS with CW and the calculated ECE for the different cases.

The contribution to the energy output for each case is mainly provided by the AD biogas (82-93-100 %), except for case 2 (HTC + DA), for which the first step of HTC produces approximately 74 % of the energy output in the form of hydrochar. The contribution from the DF H2-rich gas is rather small, being around 7 % for cases 3 and 4. In case 3, the following AD is the main contributor to the energy output (93 %).

The hydrochar mass yield produced by the HTC of F (case 4) is relatively small (5.0 % vs. 37.6 % in the CW case, as average values), and, even if the HHV of the hydrochar in the two cases is not significantly different (26.5 vs. 28.4 MJ/kg, as average), the energy output provides a rather small contribution to the total (about 11 %). Due to the poor conversion of the HTC for case 4, the substrate left for the following

Table 8
Energy outputs per 1 kg of entering TS with CW, per each step and total; calculated ECE for each case; C input/output per each step; VS input to each step.

Energy, MJ/kg of entering TS										
	Raw CW		DF	HTC			AD	TOTAL		
	TS_{in}, kg	$E_{in,CW}$	$E_{out,DF}$	$E_{out,HTC}$			$E_{out,AD}$	E_{out}		ECE %
1	1	19.76	–	–			16.22	16.22		82 %
2	1	19.76	–	10.67			3.80	14.47		73 %
3	1	19.76	0.84	–			11.73	12.57		64 %
4	1	19.76	0.84	1.29			9.38	11.51		58 %
				C, kg/kg of entering TS						
	$C_{in,CW}$ DF	$C_{out,DF}$		$C_{in,HTC}$ HTC	$C_{out,HTC}$			$C_{in,AD}$ AD	$C_{out,AD}$		CCE%
		F	gas		hydrochar	PW	gas		biogas	digestate	
1	–	–	–	–	–	–	**-**	**0.880**	0.364	0.516	41
2	–	–	–	**0.880**	0.253	0.567	0.060	0.567	0.085	0.482	38
3	**0.880**	0.834	0.046	–	–	–	–	0.834	0.263	0.571	35
4	**0.880**	0.834	0.046	0.834	0.022	0.714	0.099	0.714	0.210	0.503	32
VS, kg/kg of entering TS											
	$VS_{in,CW}$	$VS_{in,DF}$		$VS_{out,DF}$			$VS_{in,HTC}$	$VS_{out,HTC›PW}$	$VS_{in,AD}$		
1	–	–		–			–	–	**0.828**		
2	**-**	**-**		–			**0.828**	0.197	0.197		
3	**0.828**	**0.828**		0.407			–	–	0.407		
4	**0.828**	**0.828**		0.407			0.407	0.363	0.363		

Energy, MJ/kg of entering TS										
	Raw CW		DF	HTC			AD	TOTAL		
	TS_{in}, kg	$E_{in,CW}$	$E_{out,DF}$	$E_{out,HTC}$			$E_{out,AD}$	E_{out}		ECE %
1	1	19.76	–	–			16.22	16.22		82 %
2	1	19.76	–	10.67			3.80	14.47		73 %
3	1	19.76	0.84	–			11.73	12.57		64 %
4	1	19.76	0.84	1.29			9.38	11.51		58 %
				C, kg/kg of entering TS						
	$C_{in,CW}$ DF	$C_{out,DF}$		$C_{in,HTC}$ HTC	$C_{out,HTC}$			$C_{in,AD}$ AD	$C_{out,AD}$		CCE%
		F	gas		hydrochar	PW	gas		biogas	digestate	
1	–	–	–	–	–	–	**-**	**0.880**	0.364	0.516	41
2	–	–	–	**0.880**	0.253	0.567	0.060	0.567	0.085	0.482	38
3	**0.880**	0.834	0.046	–	–	–	–	0.834	0.263	0.571	35
4	**0.880**	0.834	0.046	0.834	0.022	0.714	0.099	0.714	0.210	0.503	32
VS, kg/kg of entering TS											
	$VS_{in,CW}$	$VS_{in,DF}$		$VS_{out,DF}$			$VS_{in,HTC}$	$VS_{out,HTC›PW}$	$VS_{in,AD}$		
									0.828		
1	–	–		–			–	–	0.197		
2	**-**	**-**		–			**0.828**	0.197	0.407		
3	**0.828**	**0.828**		0.407			–	–	0.363		
4	**0.828**	**0.828**		0.407			0.407	0.363			

AD step, which also has a relatively high methane specific production, produces about 82 % of the overall energy output (in the form of biogas).

In order to provide a better explanation regarding the energy outputs from the different steps, following the evolution of C and VS content might be useful, as reported in Table 8, where it is referred to one unit of mass (i.e. 1 kg) of TS entering with the raw CW.

Approximately 0.880 kg of C and 0.828 kg of VS enter with 1 kg of TS in the CW to all four systems. In case 1, all the C (and all the VS) is fed to AD and, even if the methane specific production of the raw CW is not the best one (492.1 NL/kg VS), the energy output is indicated as the highest one, as the ECE value, which is equal to 82 %. The corresponding calculated CCE is equal to 41 %, where the C non-converted into useful products remains in the AD digestate (59 %).

When HTC is applied prior to AD (case 2), a about 29 % of C is converted to hydrochar in the process, around 7 % is lost in gas, and the remaining amount in the PW is fed to AD (about 64 %), which, in turn, is converted to biogas (9.7 %) and left in the digestate (54.8 %). Overall, the C non-converted into useful products (lost in HTC gas and left in the digestate) is about 62 %. The CCE results in 38 % aligning with the ECE one and confirming that case 2 has lower efficiency than case 1. Indeed, a small amount of VS (0.197 kg, i.e. 24 % of the entering amount) is directed to the AD, which added to the lowest registered methane specific production (484.4 NL/kg TVS), generates a contained energy output contribution from AD, leading to ECE equal to 73 %.

In case 3, the C found in the H_2-rich gas is around 5 % (as already highlighted, this is in the form of CO_2), while the remaining 95 % is left in the exiting F. F, is fed to AD, where 30 % of C is converted into biogas, and the remaining 65 % is left in the digestate. Overall, the C non-converted into useful products (in this case that which remains in the digestate) is 65 %. Even if the registered methane specific production is the best one (724.8 NL/kg TVS), the lower amount of VS (equal to 0.537 kg of VS; i.e. 65 % of the entering amount) fed to AD, leads to an AD energy output lower than case 1, with a consequently lower total energy output (12.57 MJ) and ECE (64 %) than in cases 1 and 2.

In case 4, F similarly contains around 95 % of the entering C, this time fed to HTC. Hydrochar mass yield is relatively low, as already observed, with only 2 % of C converted into hydrochar. Approximately 11 % of C is lost in the gas; while about 81 % of C remains in the PW. PW is fed to AD where 24 % of C is converted into biogas, while the remaining 57 % is left in the digestate. Overall, the C non-converted into

useful products (lost in HTC gas and left in the digestate) is about 68 %. Approximately 0.463 kg of VS are fed to AD (around 56 % of the entering amount), which even if combined to the second highest methane specific production (649.5 NL/kg TVS), generates a lower energy output than in cases 1 and 3.

As the process becomes more articulated, one would expect a higher degree of recovery from the outlet streams. Counterintuitively, the ECE and the CCE decrease as the process becomes more complex. This is primarily explained by the higher rate of C non converted into useful products (lost in the gas and/or left in the digestate) highlighted for processes 2, 3 and 4, respectively 62 %, 65 % and 68 %, with respect to process 1 (59 %).

The results suggest that AD should be placed as the first steps in the chain. Indeed, when HTC is placed before AD, the overall efficiency is lower, mainly because of the C losses in the HTC gas and the low amount of TVS reaching the AD. In a worse situation, HTC seems not to be effective if applied to F. Eventually, the further possibility of overall conversion improvements should be investigated, through processing the AD digestate by HTC (out of the scope of this work), as reported in literature for food waste digestate [27] agricultural digestate [28], organic fraction of municipal solid waste digestate [29], and hemp digestate [30], but omitting the details about the energy yield of the combined process.

Additionally, placing DF before AD appears not to be beneficial in terms of overall energy output. Indeed, even if the DF operates as a pre-treatment for AD, by preparing more easily biodegradable substrates for AD, and leading to a higher methane specific production of F with respect to raw CW (724.8 vs. 492.1 NL/kg TVS) as already reported in the literature [10], the reduction (about 35 %) of VS fed to AD can lead to a lower biogas and energy production, not compensated by the H_2-rich gas production, because of the low energy yield of DF.

It should be kept in mind that these results are valid for the specific initial substrate, i.e. CW, while different substrates, with their own characteristics (VS, C, biodegradability, etc.), might require other treatment sequences, which could lead and drive to different conclusions.

4. Conclusions

Dark fermentation, anaerobic digestion and hydrothermal carbonization were applied in various combinations to CW as primary input for the different process chains, with the aim of investigating the production of individual biofuels (H_2-rich gas, biogas and hydrochar) in cascade, according to the waste biorefinery concept. The study of these integrated processes is a novel approach to assess the most effective combination in terms of energy evaluation.

The simplest case is the direct anaerobic digestion of CW, for which the methane specific production is one of the lowest (492.1 NmL/gVS), although this simple process provides the highest energy output.

Dark fermentation of cheese whey prior to its anaerobic digestion increases the specific methane production to the highest value (724.8 NmL/gVS). Similarly, the methane specific production is also improved when the dark fermentation fermentate passes through hydrothermal carbonization before being fed to anaerobic digestion (649.5 NmL/g VS, the second highest). On the contrary, hydrothermal carbonization of cheese whey produces process water in which methane specific production is not improved with respect to raw cheese whey (484.4 NmL/g VS), thus leading to the conclusion that hydrothermal carbonization is not suitable for cheese whey as an anaerobic digestion pre-treatment.

However, even if dark fermentation improves the methane specific production for the following anaerobic digestion (with or without the intermediate hydrothermal carbonization) the more complex process chains imply higher losses of volatile solids and carbon and generate a lower energy output with respect to the simplest case.

Digestate exiting the different chains still contains a non-negligible part of the entering carbon, which could be further exploited for energy purposes, suggesting that together with the previous results, and regarding maximizing energy output, anaerobic digestion should be placed as the first step of the chain and digestate could be exploited by hydrothermal carbonization, as a future development of this work.

Hydrochars produced from cheese whey and fermentate, have physical and chemical properties suitable for energy purposes confirmed by enhanced HHVs and thermal behaviour based on TG/DTG curves. However, while hydrochar yield from cheese whey is around 37–39 %, hydrochar from fermentate is only 1 – 10 %. The feedstocks were, in fact, in a liquid state and were highly organic, which was proved by high COD and Phenol index values, thus the main products of the hydrothermal carbonization process were still in the liquid organic phase providing biomethane potentials. Hydrothermal carbonization decreases by 2.5 times the COD and TOC of cheese whey, but the process water still exhibited the methane production at the same level as cheese whey. Nevertheless, this process took a further 10 days. Regarding hydrothermal effects on fermentate a contrary observation was made: COD and TOC increased 2.2 and 1.2 times, respectively, and the highest measured methane potential was found for fermentate in comparison to its process water. However, the measurements were taken on days 4 and 8 of the test. Additionally, hydrothermal carbonization caused an increase of nitrogen and ammonia in the post-processing liquid samples indicating that it could potentially be employed for agricultural uses.

Funding

The proposed process is part of a larger schematic studied within the BBCircle project founded by the Lazio Region in Italy (Avviso Pubblico “Gruppi di Ricerca 2020” Determinazione n. G08487 del July 19, 2020 U and Determinazione n. G10624 – POR FESR LAZIO 2014–2020 – Progetto n. A0375-2020-36701) and by the National Science Centre, Poland [grant no. 2021/41/B/ST8/01815].

Ethical approval

The authors declare that the work described was original research that has not been published previously, and not under consideration for publication elsewhere, in whole or in part.

Consent to publish

The manuscript is approved by all authors for publication.

CRediT authorship contribution statement

Lidia Lombardi: Writing – review & editing, Supervision, Methodology, Investigation, Funding acquisition, Conceptualization. **Shivali Sahota:** Investigation. **Alessandra Polettini:** Writing – review & editing, Supervision, Methodology, Funding acquisition. **Raffaella Pomi:** Writing – review & editing, Supervision, Methodology, Investigation, Conceptualization. **Andreina Rossi:** Methodology, Investigation. **Tatiana Zonfa:** Writing – original draft, Methodology, Investigation. **Grzegorz Cema:** Writing – original draft, Methodology, Investigation. **Klaudia Czerwińska:** Writing – original draft, Methodology, Investigation. **Aneta Magdziarz:** Writing – original draft, Methodology, Investigation. **Joanna Mikusińska:** Investigation. **Maciej Śliz:** Writing – original draft, Methodology, Investigation. **Małgorzata Wilk:** Writing – review & editing, Writing – original draft, Supervision, Methodology, Investigation, Funding acquisition, Conceptualization.

Declaration of competing interest

The authors declare that they have no known competing financial interests or personal relationships that could have appeared to influence the work reported in this paper.

Data availability

Some of experimental data are available on https://doi.org/10.58032/AGH/MDOU4S according t requirements of funder National Science Centre, Poland.

Appendix A. Supplementary data

Supplementary data to this article can be found online at https://doi.org/10.1016/j.energy.2024.132327.

References

[1] European Commission. Communication from the Commission to the European parliament, the council, the European economic and social committee and the committee of the regions; A sustainable bioeconomy for europe: strengthening the connection between economy, societya and the envi. 2018. Brussels.

[2] Cherubini F, Jungmeier G, Wellisch M, Willke T, Skiadas I, Van Ree R, et al. Toward a common classification approach for biorefinery systems. Biofuels, Bioprod Biorefining 2009;3:534–46. https://doi.org/10.1002/bbb.172.

[3] Cherubini F. The biorefinery concept: using biomass instead of oil for producing energy and chemicals. Energy Convers Manag 2010;51:1412–21. https://doi.org/10.1016/j.enconman.2010.01.015.

[4] DUBOIS J-L. Refinery of the future: feedstock, processes, products. In: Aresta M, Dumeignil F, Dibenedetto A, editors. Biorefinery. From biomass to chem. Fuels. Walter 696 gruyter GmbH Co. Berlin/Boston: KG; 2012. 2012.

[5] Schieb P-A, Lescieux-Katir H, Thénot M, Clément-Larosière B. Biorefinery 2030. Berlin, Heidelberg: Springer Berlin Heidelberg; 2015. https://doi.org/10.1007/978-3-662-47374-0.

[6] Platt R, Bauen A, Reumerman P, Geier C, Ree R Van, Gursel IV, et al. EU biorefinery outlook to 2030. https://doi.org/10.2777/103465; 2021.

[7] Alibardi L, Astrup TF, Asunis F, Clarke WP, De Gioannis G, Dessì P, et al. Organic waste biorefineries: looking towards implementation. Waste Manag 2020;114:274–86. https://doi.org/10.1016/j.wasman.2020.07.010.

[8] Carvalho F, Prazeres AR, Rivas J. Cheese whey wastewater: characterization and treatment. Sci Total Environ 2013;445–446:385–96. https://doi.org/10.1016/j.scitotenv.2012.12.038.

[9] Eurostat. Milk and milk product statistics - statistics Explained. http://epp.eurostat.ec.europa.eu/statistics_explained/index.php/Milk_and_milk_product_statistics2021; February 2014.

[10] Asunis F, De Gioannis G, Dessì P, Isipato M, Lens PNL, Muntoni A, et al. The dairy biorefinery: integrating treatment processes for cheese whey valorisation. J Environ Manag 2020;276:111240. https://doi.org/10.1016/j.jenvman.2020.111240.

[11] Asunis F, Boni MR, Brundu AP, Cappai G, Carucci A, Cocco FG, et al. Three-stage process for hydrogen and PHA production from sheep cheese whey. Sardinia, Italy 2019.

[12] Zotta T, Solieri L, Iacumin L, Picozzi C, Gullo M. Valorization of cheese whey using microbial fermentations. Appl Microbiol Biotechnol 2020;104:2749–64. https://doi.org/10.1007/s00253-020-10408-2.

[13] De Gioannis G, Muntoni A, Polettini A, Pomi R. A review of dark fermentative hydrogen production from biodegradable municipal waste fractions. Waste Manag 2013;33:1345–61. https://doi.org/10.1016/j.wasman.2013.02.019.

[14] Asunis F, De Gioannis G, Francini G, Lombardi L, Muntoni A, Polettini A, et al. Environmental life cycle assessment of polyhydroxyalkanoates production from cheese whey. Waste Manag 2021;132:31–43. https://doi.org/10.1016/j.wasman.2021.07.010.

[15] Rajesh Banu J, Ginni G, Kavitha S, Yukesh Kannah R, Adish Kumar S, Bhatia SK, et al. Integrated biorefinery routes of biohydrogen: possible utilization of acidogenic fermentative effluent. Bioresour Technol 2021;319:124241. https://doi.org/10.1016/j.biortech.2020.124241.

[16] Czerwińska K, Wierońska-Wiśniewska F, Bytnar K, Mikusińska J, Śliz M, Wilk M. The effect of an acidic environment during the hydrothermal carbonization of sewage sludge on solid and liquid products: the fate of heavy metals, phosphorus and other compounds. J Environ Manag 2024;365:121637. https://doi.org/10.1016/j.jenvman.2024.121637.

[17] Wilk M. A novel method of sewage sludge pre-Treatment-HTC. E3S Web Conf. 2016;10. https://doi.org/10.1051/e3sconf/20161000103.

[18] Wilk M, Śliz M, Czerwińska K, Śledź M. The effect of an acid catalyst on the hydrothermal carbonization of sewage sludge. J Environ Manag 2023;345:118820. https://doi.org/10.1016/j.jenvman.2023.118820.

[19] Wilk M, Gajek M, Śliz M, Czerwińska K, Lombardi L. Hydrothermal carbonization process of digestate from sewage sludge: chemical and physical properties of hydrochar in terms of energy application. Energies 2022;15:6499. https://doi.org/10.3390/en15186499.

[20] Volpe M, Fiori L. From olive waste to solid biofuel through hydrothermal carbonisation: the role of temperature and solid load on secondary char formation and hydrochar energy properties. J Anal Appl Pyrolysis 2017;124:63–72. https://doi.org/10.1016/j.jaap.2017.02.022.

[21] Saqib NU, Sharma HB, Baroutian S, Dubey B, Sarmah AK. Valorisation of food waste via hydrothermal carbonisation and techno-economic feasibility assessment. Sci Total Environ 2019;690:261–76. https://doi.org/10.1016/j.scitotenv.2019.06.484.

[22] Śliz M, Czerwińska K, Magdziarz A, Lombardi L, Wilk M. Hydrothermal carbonization of the wet fraction from mixed municipal solid waste: a fuel and structural analysis of hydrochars. Energies 2022;15:6708. https://doi.org/10.3390/en15186708.

[23] Śliz M, Tuci F, Czerwińska K, Fabrizi S, Lombardi L, Wilk M. Hydrothermal carbonization of the wet fraction from mixed municipal solid waste: hydrochar characteristics and energy balance. Waste Manag 2022;151:39–48. https://doi.org/10.1016/j.wasman.2022.07.029.

[24] Petrovič A, Cenčič Predikaka T, Škodič L, Vohl S, Čuček L. Hydrothermal co-carbonization of sewage sludge and whey: enhancement of product properties and potential application in agriculture. Fuel 2023;350:128807. https://doi.org/10.1016/j.fuel.2023.128807.

[25] Pecchi M, Baratieri M, Goldfarb JL, Maag AR. Effect of solvent and feedstock selection on primary and secondary chars produced via hydrothermal carbonization of food wastes. Bioresour Technol 2022;348:126799. https://doi.org/10.1016/j.biortech.2022.126799.

[26] Altiparmaki G, Kourletakis P, Moustakas K, Vakalis S. Assessing the effect of hydrothermal treatment (HT) severity on the fate of nitrates and phosphates in dairy wastewater. Fuel 2022;312:122866. https://doi.org/10.1016/j.fuel.2021.122866.

[27] Yan M, Chen F, Li T, Zhong L, Feng H, Xu Z, et al. Hydrothermal carbonization of food waste digestate solids: effect of temperature and time on products characteristic and environmental evaluation. Process Saf Environ Protect 2023;178:296–308. https://doi.org/10.1016/j.psep.2023.08.010.

[28] Mikusińska J, Kuźnia M, Czerwińska K, Wilk M. Hydrothermal carbonization of digestate produced in the biogas production process. Energies 2023;16:5458. https://doi.org/10.3390/en16145458.

[29] Pawlak-Kruczek H, Urbanowska A, Niedzwiecki L, Czerep M, Baranowski M, Aragon-Briceño C, et al. Hydrothermal carbonisation as treatment for effective moisture removal from digestate—mechanical dewatering, flashing-off, and condensates' processing. Energies 2023;16:5102. https://doi.org/10.3390/en16135102.

[30] Farru G, Asquer C, Cappai G, De Gioannis G, Melis E, Milia S, et al. Hydrothermal carbonization of hemp digestate: influence of operating parameters. Biomass Convers Biorefinery 2022. https://doi.org/10.1007/s13399-022-02831-4.

[31] APHA AWWA, WEF. Standard methods for the examination of water and wastewater. 23rd Edition 2017.

[32] DuBois M, Gilles KA, Hamilton JK, Rebers PA, Smith F. Colorimetric method for determination of sugars and related substances. Anal Chem 1956;28:350–6. https://doi.org/10.1021/ac60111a017.

[33] Channiwala SA, Parikh PP. A unified correlation for estimating HHV of solid, liquid and gaseous fuels. Fuel 2002;81:1051–63. https://doi.org/10.1016/S0016-2361(01)00131-4.

[34] Wang B, Nges IA, Nistor M, Liu J. Determination of methane yield of cellulose using different experimental setups. Water Sci Technol 2014;70:599–604. https://doi.org/10.2166/wst.2014.275.

[35] Holliger C, Alves M, Andrade D, Angelidaki I, Astals S, Baier U, et al. Towards a standardization of biomethane potential tests. Water Sci Technol 2016;74:2515–22. https://doi.org/10.2166/wst.2016.336.

[36] Lehtomäki A, Huttunen S, Rintala JA. Laboratory investigations on co-digestion of energy crops and crop residues with cow manure for methane production: effect of crop to manure ratio. Resour Conserv Recycl 2007;51:591–609. https://doi.org/10.1016/j.resconrec.2006.11.004.

[37] Lombardi L, Polettini A, Pomi R, Rossi A, Czerwińska K, Śliz M, et al. Hydrothermal carbonization as part of the biorefining of cheese whey. 7th int. Conf. Contemp. Probl. Therm. Eng. Towar. Sustain. Decarbonized energy syst. Warsaw, Poland, 20-23 sept. 2022 conf. Proc.; 2022. p. 581–91.

[38] Wang R, Wang C, Zhao Z, Jia J, Jin Q. Energy recovery from high-ash municipal sewage sludge by hydrothermal carbonization: fuel characteristics of biosolid products. Energy 2019;186:115848. https://doi.org/10.1016/j.energy.2019.07.178.

[39] Shrestha A, Acharya B, Farooque AA. Study of hydrochar and process water from hydrothermal carbonization of sea lettuce. Renew Energy 2021;163:589–98. https://doi.org/10.1016/j.renene.2020.08.133.

[40] Xiao H, Zhai Y, Xie J, Wang T, Wang B, Li S, et al. Speciation and transformation of nitrogen for spirulina hydrothermal carbonization. Bioresour Technol 2019;286:121385. https://doi.org/10.1016/j.biortech.2019.121385.

[41] Wang X, Esquerre C, Downey G, Henihan L, O'Callaghan D, O'Donnell C. Feasibility of discriminating dried dairy ingredients and preheat treatments using mid-infrared and Raman spectroscopy. Food Anal Methods 2018;11:1380–9. https://doi.org/10.1007/s12161-017-1114-9.

[42] Chatzipaschali AA, Stamatis AG. Biotechnological utilization with a focus on anaerobic treatment of cheese whey: current status and prospects. Energies 2012;5:3492–525. https://doi.org/10.3390/en5093492.

[43] Labatut RA, Angenent LT, Scott NR. Biochemical methane potential and biodegradability of complex organic substrates. Bioresour Technol 2011;102:2255–64. https://doi.org/10.1016/j.biortech.2010.10.035.

[44] Escalante H, Castro L, Amaya MP, Jaimes L, Jaimes-Estévez J. Anaerobic digestion of cheese whey: energetic and nutritional potential for the dairy sector in

developing countries. Waste Manag 2018;71:711–8. https://doi.org/10.1016/j.wasman.2017.09.026.
[45] Real Olvera J del, Lopez-Lopez A. Biogas production from anaerobic treatment of agro-industrial wastewater. Biogas: InTech; 2012. https://doi.org/10.5772/31906.
[46] Antonopoulou G, Stamatelatou K, Venetsaneas N, Kornaros M, Lyberatos G. Biohydrogen and methane production from cheese whey in a two-stage anaerobic process. Ind Eng Chem Res 2008;47:5227–33. https://doi.org/10.1021/ie071622x.